How Intense is Parametric X Radiation?

S. Asano, I. Endo,[a] M. Harada, S. Ishii, T. Kobayashi, and T. Nagata
Faculty of Science, Hiroshima University, Kagamiyama, Higashi-Hiroshima 724, Japan

M. Muto and K. Yoshida
Institute for Nuclear Study, University of Tokyo, Tanashi, Tokyo 188, Japan

H. Nitta
Department of Physics, Tokyo Gakugei University, Koganei, Tokyo 184, Japan
(Received 5 March 1993)

We have measured the crystal-angle dependence and the intensity of the parametric x radiation from a Si single crystal impinged upon by an electron beam with the energy ranging from 200 to 1100 MeV. It has been found that the x-ray intensity is higher and the angular spread is less broad than the predictions of the theoretical model due to Feranchuk and Ivashin. This calls for a more elaborate theoretical treatment of multiple scattering, and encourages research aiming at a new type of x-ray source based on the parametric x-radiation mechanism.

PACS numbers: 42.25.Fx, 78.90.+t

Parametric x radiation (PXR) is emitted into a small angular cone approximately satisfying the Bragg condition for x-ray diffraction, when a relativistic charged particle passes through crystal planes. It can be intuitively understood as Bragg diffraction of virtual photons associated with the incident particle. Although there have been several theoretical works on PXR [1–6] since the first consideration by Ter-Mikaerian [7], the existence of PXR had not been confirmed experimentally until the pioneering work at Tomsk [8]. Most of the experimental results obtained up to now [8–12] are qualitatively consistent with the existing theory under the kinematical approximation.

Remarkable features of PXR are as follows: (1) It is a monochromatic x-ray source with continuously variable wavelength. (2) It is emitted to the direction well separated from the electron beam. (3) The angular and energy spread of x rays are expected to be of the order of $1/\gamma$, where γ stands for the energy to mass ratio of the incident electron. (4) The x-ray energy and the total photon numbers are virtually independent from the electron beam energy. They suggest that PXR can be an excellent x-ray source provided the number of photons generated by a single passage of high-energy electron is large enough. Is it possible to use a thick crystal to generate a high-brilliance x-ray beam comparable to the synchrotron radiation from a typical storage ring?

In order to more quantitatively study the characteristics of PXR, it is necessary to consider the effects of the electron multiple scattering (EMS) and photon absorption in the target crystal. Feranchuk and Ivashin (Ref. [2]) have phenomenologically incorporated the effects of EMS and photon absorption into the theory of PXR, hereafter referred to as the FI model. Their formula of the differential intensity for a single reciprocal lattice vector $\boldsymbol{h}$ is written as

$$\frac{\partial^2 N}{\partial\theta_x \partial\theta_y} = \frac{\alpha}{4\pi}\omega_B Z \frac{|g_{\boldsymbol{h}}|^2}{\sin^2\theta_B}\frac{\theta_x^2\cos^2 2\theta_B + \theta_y^2}{(\theta_x^2+\theta_y^2+\theta_{ph}^2)^2}, \tag{1}$$

where

$$Z = L_a\left[1-\exp\left(-\frac{L_c}{L_a}\right)\right], \quad \theta_{x,y} = \frac{(\boldsymbol{k}-\boldsymbol{k}_B)_{x,y}}{\omega_B},$$

$$\theta_{ph}^2 = \frac{1}{\gamma^2} + \theta_s^2 - \mathrm{Re}g_0, \quad \theta_s = \frac{21\ \mathrm{MeV}}{E_e}\sqrt{\frac{L_c}{L_R}}.$$

Here L_a, L_c, and L_R are the absorption length, thickness, and radiation length of the target crystal, respectively. The electron mass is denoted by m_e, the photon momentum by $\boldsymbol{k}$, and the fine structure constant by α. The quantity $g_{\boldsymbol{h}}$ is the Fourier component of the electric susceptibility. The angle θ_B is defined by half the detection angle θ_D measured from the beam direction, and can be looked upon as Bragg angle of the virtual photon diffraction. The vector $\boldsymbol{k}_B$ is in the plane defined by the incident electron direction and $\boldsymbol{h}$. It has a magnitude, $|\boldsymbol{k}_B| = \omega_B$, satisfying the relation $\omega_B \sin\theta_B = |\boldsymbol{h}|/2$. The axes x and y are in horizontal and vertical direction, respectively, in the plane perpendicular to $\boldsymbol{k}_B$. The quantity Z is regarded as an effective thickness of the crystal corrected for the x-ray absorption.

In the FI model, the absorption process does not affect the emission mechanism of PXR and only reduces the number of produced photons. On the other hand, the EMS is treated as fully coherent with the PXR mechanism. It affects θ_{ph}, the intrinsic angular spread of PXR, and consequently the number of photons emitted in a given solid angle.

In order to evaluate the validity of the FI model, we systematically measured the crystal-angle dependence of the PXR intensity for the electron energies between 300 and 1100 MeV. The absolute intensity of PXR, i.e., the number of photons emitted by a single electron, were also measured for the same purpose.

The experiment was performed by using the 1.3 GeV electron synchrotron at the Institute for Nuclear Study, University of Tokyo. The target crystal was a monocrystalline silicon plate with the size $17 \times 17 \times 0.5$ mm^3. The surface of the plate and one of the edges were in normal to the crystallographic axis $[\bar{1}10]$ and [111], respectively. The target was mounted on a three axis computer controlled goniometer whose angular resolution was about 0.004°. The electron beam extracted from the synchrotron entered the target crystal with an incident angle θ relative to the (111) crystallographic plane. An NaI scintillation counter [EG&G ORTEC model 286: a 1 mm thick, 25.4 mm diam NaI(Tl) single crystal with 0.13 mm thick Be entrance window, attached with the RCA4523 photomultiplier tube], referred to as X counter, was used as an x-ray detector. It was placed at 192.5 cm from the target and covered the solid angle 9.12×10^{-5} sr around the emission angle $\theta_D = 2\theta_B$ relative to the electron beam direction. The detection efficiency was measured by using a standard x-ray source ^{57}Co, of which the intensity was known to the accuracy of $\pm 3.8\%$, and found to be $(73\pm4)\%$ including the effect of x-ray absorption in the air at x-ray energy 14.4 keV. The energy resolution at 14.4 keV was 9.3% (1σ). We chose the detection angle $\theta_D = 15.78°$ in order to make the peak energy of the (111) reflection coincide with 14.4 keV at which we know the detection efficiency. The number of electrons passing through the target crystal was monitored by a plastic scintillation counter, referred to as N counter, and by a thick walled ionization chamber installed downstream from the target crystal. Another plastic scintillation counter, V counter, having a 13 mm diam hole in the center was placed 5 cm upstream from the target in order to obtain the information of the beam halo. The target and the detector system were set in the air and the electron beam extracted from the vacuum chamber of the synchrotron hit the target after passing through the 244 cm air. The exit window of the vacuum chamber is a 100 μm thick Mylar sheet.

A typical pulse-height distribution of the X counter without background subtraction at electron energy $E_e =$ 1100 MeV is shown in Fig. 1. We see clear peaks for the (111), (333), and (444) reflections. The forbidden (222) reflection peak does not show up. A fit with a Gaussian function for the (111) peak gives the peak position $14.60\pm$ 0.02 keV which is very close to the expected value 14.4 keV for the perfect geometry.

The crystal-angle dependence of PXR, hereafter referred to as θ scan, was measured at E_e=300, 700, and 1100 MeV by varying the crystal angle θ in the range $|\theta - \theta_B| < 2°$ for fixed detection angle θ_D. By using a single-channel analyzer, we counted signals with pulse height falling in the range between the two arrows shown in Fig. 1 in order to determine the photon numbers belonging to the (111) reflection. We found that the θ-scan curve has a maximum at $\theta = \theta_B$ and rapidly falls off until it reaches the constant background level at around $|\theta - \theta_B| = 1.5°$. A background to peak ratio was 14% at $E_e = 300$ MeV and 3.2% at $E_e = 1100$ MeV. The obtained results for the θ scan, after the background subtraction, are compared with the prediction of the FI model in Fig. 2. The solid curves were obtained by integrating the FI formula (1) over the detector solid angle for each θ point using a Monte Carlo (MC) technique. The angular and spatial spread of the initial electron beam were taken into account in the MC calculation as described later. We notice that the experimental results are more sharply peaked than the theoretical curves at all energies. The discrepancies are the most striking at the lowest energy; the experimental width is even smaller than the dot-dashed curve in Fig. 2(a) which shows the FI model applied for a fictitious case where the incident beam has no angular divergence at all.

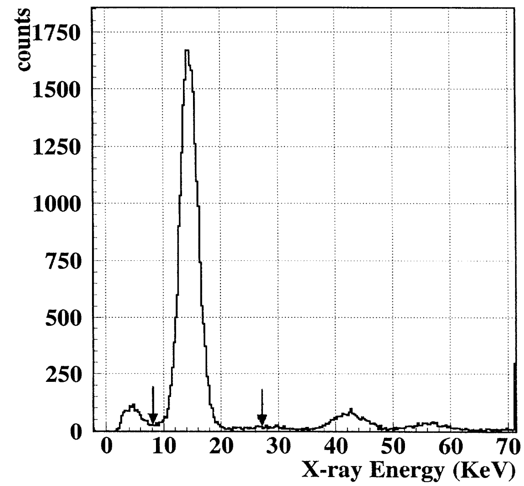

FIG. 1. A typical spectrum of PXR at electron energy 1100 MeV. The upper and lower discrimination levels for counting the PXR photons belonging to the (111) reflection peak are shown by the arrows.

In order to increase an accuracy of the absolute intensity measurement, we took the following precautions.

(1) The electron beam intensity was reduced to $\sim 10^5$/s to prevent the counting loss due to pulse pileup effect in the N counter. We then confirmed that the ratio of the X to N counts did not alter within the 10% accuracy, when the electron beam intensity was changed by $\pm 50\%$.

(2) The contribution from the bremsstrahlung upstream was estimated by placing a 1.1 mm thick aluminum plate in the electron beam line. The obtained ratios X/N with and without the Al plate were $(1.13 \pm 0.03) \times 10^{-5}$ and $(1.17 \pm 0.03) \times 10^{-5}$, respectively. This verified that we were predominantly counting the PXR.

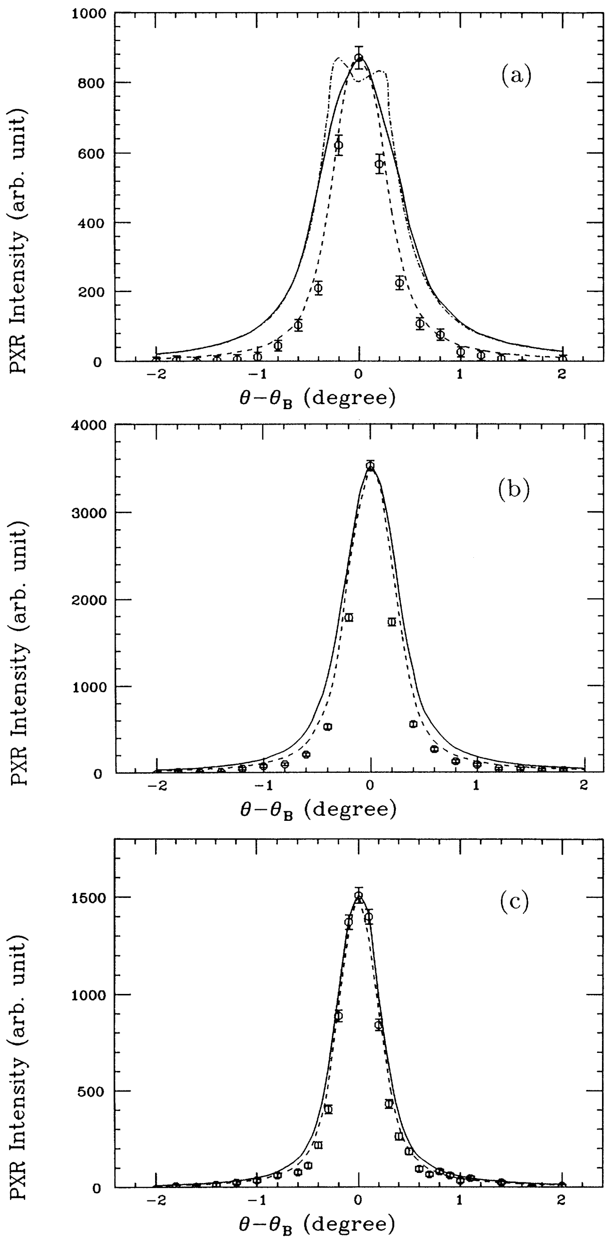

FIG. 2. Relative intensities of PXR are plotted by circular points as a function of deviation of crystal angle from the Bragg angle θ_B. (a), (b), and (c) are for the electron energies 300, 700, and 1100 MeV, respectively. The theoretical predictions, normalized to the experimental value at the peak, of the FI model are shown by solid curves, while those of the incoherent model are shown by dashed curves. The dot-dashed curve in (a) shows the FI model without beam divergence.

It is necessary to estimate the number of electrons which actually hit the target, because the N counter is larger than the crystal size. Since the beam shape was not directly measured, we made a MC simulation in which the multiple scattering of the electrons in the Mylar window and the air is taken into account. We determined the parameters of the beam shape at the exit of the electron extraction channel so as to reproduce the observed ratio $r = N \otimes \overline{V}/N$. The quantity $N \otimes \overline{V}$ denotes the number of pulses from the N counter unaccompanied by a coincident pulse from the V counter. It represents the number of electrons passing through the hole of the V counter. The most probable number of hitting electrons $N_{\rm hit}$ was obtained by calculating the probability for an electron to hit the crystal by using the beam parameters thus obtained.

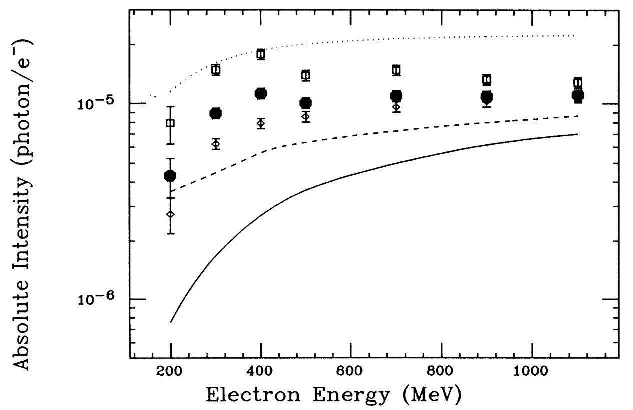

FIG. 3. The electron energy dependence of the PXR photon numbers accepted by the detector solid angle 9.12×10^{-5} sr for $\theta = \theta_B$. The experimental values are plotted by solid circles. The solid and dashed curves are the theoretical predictions of the FI and incoherent model, respectively. The dotted line shows the theoretical calculation neglecting the beam divergence, EMS, and photon absorption in the crystal. The points marked by rhombuses and squares indicate the maximum range of errors due to the ambiguity of the beam shape.

At high electron energies, the beam size is small enough so that the ratio r is close to unity and we can reliably determine the absolute intensity without recourse to the MC simulation. In fact, the ratio was found to be 0.84 at E_e=1100 MeV, and we regarded $N - N_{\rm hit}$ and $N \otimes \overline{V} - N_{\rm hit}$ counts as the upper and lower limits, respectively, of the error of $N_{\rm hit}$ to obtain the absolute intensity; $(11.1^{+2.5}_{-1.0}) \times 10^{-6}$ photon/e^-. The PXR intensities for all energies determined by using the MC-estimated $N_{\rm hit}$ are plotted by solid circles in Fig. 3. It is readily seen that they do not appreciably change with the electron energy at $E_e > 300$ MeV. The points marked by rhombuses and squares are calculated by tentatively taking the N and $N \otimes \overline{V}$ as the number of electrons passing through the target. They indicate the lower and upper bound of errors due to the ambiguity in the beam shape. In Fig. 3 is also drawn the prediction of the FI model by a solid curve in which the angular and spatial spread of the incident beam were taken into account. We see that the predicted intensity is more strongly dependent on E_e

than the experimental results, and that it is too small at all electron energies: The theoretical values at E_e=300 and 1100 MeV are 0.19 and 0.63 times the experimental one, respectively.

The discrepancies found here are apparently caused by the energy-dependent angular spread θ_{ph} in formula (1) which is dominated by θ_s in the present experimental condition. We tried another model (incoherent model) in order to clarify the effect of the term θ_s in θ_{ph}. In the incoherent model, the EMS is assumed not to affect the intrinsic angular spread of PXR, i.e., $\theta_s = 0$ in the formula (1), but is treated as an angular fluctuation of the incident electron beam. The predictions of the incoherent model for the absolute intensity and the θ scan are drawn by dashed curves in Figs. 3 and 2, respectively. They are less dependent on the electron energy than those for the FI model and closer to the experimental results, thus indicating that the EMS in the crystal is not to be treated as fully coherent with the emission mechanism of PXR.

The dotted curve in Fig. 3 shows the theoretical calculation for the ideal case, i.e., the case where the incident beam divergence, the EMS, and the photon absorption can be neglected. The experimental values lie in between the incoherent model and the ideal case. This suggests that the photon absorption mechanism, too, is not as simple as the one assumed in the FI model.

In a more sophisticated theory by Baryshevsky, Grubich, and Hai [3], no quantitative prediction is made for the case of a thick crystal, while the EMS is treated in a similar way as in the FI model for a thin crystal with $L_c \leq L_{BS}$ where L_{BS} is the coherent length of bremsstrahlung, $L_{BS} = (2/\theta_s)\sqrt{L_c/\omega_B}$. Being $L_c \geq 5L_{BS}$, the present experimental condition is out of scope of Baryshevsky's formula. It is to be noted, however, that if we considered the crystal as consisting of many plates with thickness L_{BS} and incoherently summed up the radiation intensity from each plate calculated by Baryshevsky's thin-crystal formula, the obtained results would behave like our incoherent model.

To summarize, we have found that the parametric x rays are more intense and more collimated than the theoretical calculation based on the FI model. This means that more subtle theoretical treatment of electron multiple scattering and photon absorption in the crystal is necessary.

For possible practical applications of PXR, the present results are quite encouraging; it is worth trying a very thick crystal to generate a high intensity x-ray beam. Further study with various crystal thicknesses and materials is desirable.

(a) To whom correspondence should be addressed.

[1] V.G. Baryshevsky and I.D. Feranchuk, J. Phys. (Paris) **44**, 913 (1983).

[2] I.D. Feranchuk and A.V. Ivashin, J. Phys. (Paris) **46**, 1981 (1985).

[3] V.G. Baryshevsky, A.O. Grubich, and Le Tien Hai, Zh. Eksp. Teor. Fiz. **94**, 51 (1988) [Sov. Phys. JETP **67**, 895 (1988)].

[4] H. Nitta, Phys. Lett. A **158**, 270 (1991).

[5] H. Nitta, Phys. Rev. B **45**, 7621 (1992).

[6] A. Caticha, Phys. Rev. B **45**, 9541 (1992).

[7] M.L. Ter-Mikaerian, *High-Energy Electromagnetic Processes in Condensed Media* (Wiley-Interscience, New York, 1972).

[8] S.A. Vorob'ev, B.N. Kalinin, S. Pak, and A.P. Potylitsyn, Pis'ma Zh. Eksp. Teor. Fiz. **41**, 3 (1985) [JETP Lett. **41**, 1 (1985)].

[9] Yu.N. Adishchev *et al.*, Nucl. Instrum. Methods Phys. Res., Sect. B **44** 130 (1989).

[10] Yu.N. Adishchev *et al.*, Phys. Lett. **A 147** 326 (1990).

[11] K.Yu. Amosov *et al.*, Phys. Rev. E **47**, 2207 (1993).

[12] Yu.N. Adishchev *et al.*, Nucl. Instrum. Methods Phys. Res., Sect. B **21** 49 (1987).